Inorg. Chem. **2007**, *46*, 4120–4127

Heterobimetallic Molecular Cages for the Deposition of Cu/Ti and Cu/Zn Mixed-Metal Oxides

Mazhar Hamid,[†] Asif A. Tahir,[†] Muhammad Mazhar,*[,†] Matthias Zeller,[‡] and Allen D. Hunter[‡]

Department of Chemistry, Quaid-I-Azam University, Islamabad 45320, Pakistan, and STaRBURSTT-Cyberdiffraction Consortium at YSU and Department of Chemistry, Youngstown State University, 1 University Plaza, Youngstown, Ohio 44555-3663

Received December 21, 2006

Heterobimetallic molecular precursors $[Ti_4(dmae)_6(\mu\text{-}OH)(\mu\text{-}O)_6Cu_6(OAc)_8{\cdot}H_2O]$ (**1**) and $[Zn_7(OAc)_{10}(\mu\text{-}OH)_6Cu_5(dmae)_4Cl_4]$ (**2**) for the deposition of metal oxide thin films of $Cu_6Ti_4O_{12}$ (Cu_3TiO_4, TiO_2) and $Cu_5Zn_7O_{12}$ (ZnO, CuO) were prepared by the interaction of $Ti(dmae)_4$ with $Cu(OAc)_2{\cdot}2H_2O$ for **1** and tetrameric (*N*,*N*-dimethylamino)-ethanolatocopper(II) chloride, $[(dmae)CuCl]_4$ [where dmae = (*N*,*N*-dimethylamino)ethanolate] with $Zn(OAc)_2{\cdot}2H_2O$ (where OAc = acetate) for **2** in dry toluene. Both complexes were characterized by melting point, elemental analysis, Fourier transform IR, fast atom bombardment mass spectrometry, thermal analysis (TGA), and single-crystal X-ray diffraction. TGA and XRD prove that complexes **1** and **2** undergo facile thermal decomposition at 300 and 460 °C to form thin films of Cu/Ti and Cu/Zn mixed-metal oxides, respectively. Scanning electron microscopy and XRD of the thin films suggest the formation of impurity-free crystallite mixtures of Cu_3TiO_4 and TiO_2, with average crystallite sizes of 22.2 nm from complex **1** and of ZnO and CuO with average crystallite sizes of 26.1 nm from complex **2**.

Introduction

The composition and microstructure of solid-state materials determine their properties, thus making factors that control their composition and structure crucial for the preparation of solids with those desired properties. A wide range of different flexible synthetic routes has been employed for the development of complex nanometer-scale materials with tunable properties able to satisfy the ever-changing technological demands. One of the most promising approaches toward the synthesis of these kinds of mixed-metal oxides is the use of single-source precursors (SSPs).[1−7]

Because of their outstanding electrical properties, many $MTiO_3$-type perovskites (where M = Ca, Sr, Ba, Pb, Cu) or their solid solutions are key materials of critical components in a range of electronic devices.[8] Although these oxides have been used for more than 50 years, unusual features have only recently been found for their ferroelectric and piezoelectric properties that might lead to new technological applications for these compounds.[9,10] Specifically, the discovery of a giant dielectric constant in $CaCu_3Ti_4O_{12}$ has shifted renewed interest toward perovskite-type oxides.[11−13] Similarly, non-stoichiometric oxides of the type $MTiO_3$ (M = Ni, Fe, Co, Mn, Cu, Zn) have been studied as functional inorganic materials with wide applications such as electrodes of solid oxide fuel cells, metal−air barriers, gas sensors, and high-performance catalysts.[14−16] The Cu/ZnO system is of much importance in the large-scale industrial Fisher−Tropsch-type synthesis.[17]

* To whom correspondence should be addressed. E-mail: mazhar42pk@yahoo.com.
[†] Quaid-I-Azam University.
[‡] Youngstown State University.

(1) Veith, M. *Dalton Trans.* **2002**, 2405−2412.
(2) Kessler, V. G. *Chem. Commun.* **2003**, 1213−1222.
(3) Hubert-Pfalzgraf, L. G. *Coord. Chem. Rev.* **1998**, *180*, 967−997.
(4) Mehrotra, R. C.; Singh, A.; Sogani, S. *Chem. Rev.* **1994**, *94*, 1643−1660.
(5) Ertl, G.; Knözinger, H.; Weitkamp, J. *Handbook of Heterogeneous Catalysis*; Wiley-VCH: Weinheim, Germany, 1997.
(6) Polarz, S.; Orlov, A. V.; van den Berg, M. W. E.; Driess, M. *Angew. Chem., Int. Ed.* **2005**, *44*, 7892−7896.
(7) Vieth, M.; Mathur, S.; Huch, V. *Inorg. Chem.* **1997**, *36*, 2391−2399.
(8) Moulson, A. J.; Herbert, J. M. *Electroceramics: Materials, Properties and Applications*, 2nd ed.; Wiley: New York, 2003.
(9) Chu, M.-W.; Szafraniak, I.; Scholz, R.; Harnagea, C.; Hesse, D.; Alexe, M.; Gosele, U. *Nat. Mater.* **2004**, *3*, 87−90.
(10) Ren, X. *Nat. Mater.* **2004**, *3*, 91−94.
(11) Subramanian, M. A.; Duan, N.; Reisner, B. A.; Sleight, A. W. *J. Solid State Chem.* **2000**, *151*, 323−325.
(12) Ramirez, A. P.; Subramanian, M. A.; Gardel, M.; Blumberg, G.; Li, D.; Vogt, T.; Shapiro, S. M. *Solid State Commun.* **2000**, *115*, 217−220.
(13) Homes, C. C.; Vogt, T.; Shapiro, S. M.; Wakimoto, S.; Ramirez, A. P. *Science* **2001**, *293*, 673−676.

10.1021/ic0624470 CCC: $37.00
Published on Web 04/20/2007

Recently, many researchers started to extensively work on the development of heterobimetallic complexes of Cu with Ti and Zn, but none of the investigated complexes were used for the deposition of mixed-metal oxides. Typical examples, among many others, are $[Cu_2Zn(NH_3)I_3(Me_2Ea)_3]$,[18] $[[CuZnBPFP(\mu\text{-}OH)](ClO_4)_2]$,[19] $[[Cu(en)_2ZnX_4]\cdot(Solv)]$,[20] $[[(CuimZnL_{2H})(CuimZnL_H)](ClO_4)_3]$,[21] $[(Me_3Si)_3CZnCl\cdot Cu(OCH(R)CH_2NMe_2)_2]$,[22] $[ClCu[Ti_2(OPr^i)_9]$,[23] $[(C_5H_5)_2Ti[SCH_2CH_2P(C_6H_5)_2Cu]BF_4]$,[24] and $[[(C_5H_5)_2Ti(\mu\text{-}SCH_2CH_3)_2CuL]PF_6]$.[25]

We were attracted by this idea and selected the Cu/Ti and Cu/Zn mixed-metal oxide system as a focus of our studies. This led us to investigate the possibility of developing soluble and volatile metalloorganic SSPs for the preparation of mixed-metal oxide systems. Following our previous work directed toward the design of heterobimetallic complexes for mixed-metal oxide systems, we took advantage of aminoalcohol ligands such as (*N*,*N*-dimethylamino)ethanol (dmaeH) that can coordinate in several ways and often allow the formation of soluble high-nuclearity species.[26−28] The reaction of $Ti(dmae)_4$ with copper(II) acetate dihydrate, $Cu(OOCH_3)_2\cdot 2H_2O$, gave crystalline $[Ti_4(dmae)_6(\mu\text{-}OH)(\mu\text{-}O)_6Cu_6(OAc)_9\cdot H_2O\cdot 1.5(C_6H_7-CH_3)]$ (**1**), while tetrameric (*N*,*N*-dimethylamino)ethanolatocopper(II) chloride, $[(dmae)CuCl]_4$, reacts under very mild conditions with zinc(II) acetate dihydrate, $Zn(OOCH_3)_2\cdot 2H_2O$, to give $[Zn_7(OAc)_{10}(\mu\text{-}OH)_6Cu_5(dmae)_4Cl_4\cdot 2(C_6H_7-CH_3)]$ (**2**). Both cage complexes **1** and **2** are highly soluble under experimental conditions of aerosol-assisted chemical vapor deposition and deposit homogeneous thin films of Cu/Ti and Cu/Zn mixed-metal oxides with possible uses in industrial and other technological applications.

Experimental Section

All manipulations were carried out under an inert atmosphere of dry Ar using Schlenk tube and glovebox techniques. Solvents were rigorously dried and distilled over sodium metal/benzophenone. $Zn(OAc)_2\cdot 2H_2O$, $Cu(OAc)_2\cdot 2H_2O$, Li metal, and $Ti(OC_2H_5)_4$ were purchased from Aldrich Chemicals and were stored in a glovebox under Ar. $Ti(dmae)_4$ and $[Cu(dmae)Cl)]_4$ were prepared by literature procedures.[29,30] All other reagents were purchased from Fluka Chemicals. Melting points were recorded on a Mitamura Riken Kogyo (MT-D) apparatus and are uncorrected. Elemental analyses were performed using a LECO model CHNS-932 CHN analyzer. Fast atom bombardment mass spectrometry (FABMS) spectra were recorded using a JMS-HX-1100 mass spectrometer from JEOL, Japan. Fourier transform IR (FT-IR) spectra were recorded as KBr disks with a Spectrum-1000 from Perkin-Elmer. Magnetic measurements were made using a commercial model BHV-50 vibrating sample magnetometer, Perkin Denshi Co. (Ltd.), Japan.

Controlled thermal analyses (TGA) of the complexes were investigated using a Perkin-Elmer TGA-7 thermogravimetric analyzer with a computer interface. The measurements were carried out in an alumina crucible under an atmosphere of flowing N_2 gas (25 mL/min) at a heating rate of 10 °C/min.

Scanning electron microscopy (SEM) was carried out using a JEOL JSM-5910 scanning electron microscope with a Be window. Metallic elemental ratios were recorded on an Inca-200 EDX analyzer from Oxford Instruments, U.K. X-ray diffraction (XRD) peak patterns of the thin films were collected using a PANanalytical, X'Pert PRO diffractometer with Cu Kα radiation.

Single-crystal XRD data of complexes **1** and **2** were collected on a Bruker AXS SMART APEX CCD diffractometer at 100(2) K using monochromatic Mo Kα radiation with the ω scan technique. The unit cells were determined using *SAINT*+, and the data were corrected for absorption using *SADABS* in *SAINT*+.[31] The structures were solved by direct methods and refined by full-matrix least squares against F^2 with all reflections using *SHELXTL*.[32] Refinement of extinction coefficients was found to be insignificant. All non-H atoms were refined anisotropically.

For complexes **1** and **2**, all hydroxyl H atoms were located in the difference density Fourier map and were refined with an isotropic displacement parameter 1.2 times that of the adjacent O atom. The O−H distances were restrained to be 0.82 Å within a standard deviation of 0.01. Water H atoms in **1** were also located in the difference density Fourier map and were refined with an isotropic displacement parameter 1.5 times that of the adjacent O atom. The O−H distances were restrained to be 0.90 Å within a standard deviation of 0.02. All other H atoms were placed in calculated positions and were refined with an isotropic displacement parameter 1.2 (C−H and CH_2) or 1.5 (CH_3) times that of the adjacent C atom.

In complex **2**, one of the metal sites (Zn3/Cu3) was refined as disordered between Cu and Zn with an equal occupancy ratio within the margin of accuracy (refined value: 0.47(4) for Zn to 0.53(4) for Cu). The coordinates as well as the anisotropic displacement parameters of Zn3 and Cu3 were restrained to be identical. This action seems to be justified by the following observations: Refining all metal atoms with an additional free variable for occupancy results in only the Zn3/Cu3 site being questionable. All other metal sites are unambiguously either Cu or Zn. Fixing the site in question as either Cu or Zn has no large effect on the final *R* values, but in

(14) Dharmaraj, N.; Park, H. C.; Kim, C. K.; Kim, H. Y.; Lee, D. R. *Mater. Chem. Phys.* **2004**, *87*, 5−9.
(15) Tohji, K.; Udagawa, Y.; Tanabe, S.; Ida, T.; Ueno, A. *J. Am. Chem. Soc.* **1984**, *106*, 5172−5186.
(16) Kim, D.-U.; Gong, M.-S. *Sens. Actuators B* **2005**, *110*, 321−326.
(17) Cybulski, A. *Catal. Rev. Sci. Eng.* **1994**, *36*, 557−562.
(18) Vinogradova, E. A.; Vassilyeva, O. Yu.; Kokozay, V. N. *Inorg. Chem. Commun.* **2002**, *5*, 19−22.
(19) Torelli, S.; Belle, C.; Gautier-Luneau, I.; Hamman, S.; Pierre, J.-L. *Inorg. Chim. Acta* **2002**, *333*, 144.
(20) Pryma, O. V.; Petrusenko, S. R.; Kokozay, V. N.; Skelton, B. W.; Shishikin, O. V.; Teplytska, T. S. *Eur. J. Inorg. Chem.* **2003**, *7*, 1426−1432.
(21) Lie, D.; Lie, S.; Yang, D.; Yu, J.; Huang, J.; Lie, Y.; Tang, W. *Inorg. Chem.* **2003**, *42*, 6071−6080.
(22) Becker, R.; Jurij, W.; Manuela, W.; Klaus, M.; Roland, A. F. *J. Organomet. Chem.* **2001**, *630*, 253−262.
(23) Vieth, M.; Mathur, S.; Huch, V. *Inorg. Chem.* **1997**, *36*, 2391−2399.
(24) White, G. S.; Stephan, D. W. *Inorg. Chem.* **1985**, *24*, 1499−1503.
(25) Wark, T. A.; Stephan, D. W. *Inorg. Chem.* **1987**, *26*, 363−369.
(26) Ribas, J.; Monfort, M.; Costa, R.; Solans, X. *Inorg. Chem.* **1993**, *32*, 695−699.
(27) El Fallah, M. S.; Rentschler, E.; Caneschi, A.; Sessoli, R.; Gatteschi, D. *Inorg. Chem.* **1996**, *35*, 3723−3724.
(28) Tahir, A. A.; Molloy, K. C.; Mazhar, M.; Kociok-Köhn, G.; Hamid, M.; Dastgir, S. *Inorg. Chem.* **2005**, *44*, 9207−9212.
(29) Johnson, B. F. G.; Klunduk, M. C.; O'Connell, T. J.; McIntosh, C.; Ridland, J. *J. Chem. Soc., Dalton Trans.* **2001**, *10*, 1553−1555.
(30) Hamid, M.; Tahir, A. A.; Mahzar, M.; Zeller, M.; Hunter, A. D. *Inorg. Chem.* **2006**, *45*, 10457−10466.
(31) Bruker Advanced X-ray Solutions. *SAINT*, version 6.45; Bruker AXS Inc.: Madison, WI, 1997−2003.
(32) (a) Bruker Advanced X-ray Solutions. *SMART for WNT/2000*, version 5.628; Bruker AXS Inc.: Madison, WI, 1997−2002. (b) Bruker Advanced X-ray Solutions. *SHELXTL*, version 6.10; Bruker AXS Inc.: Madison, WI, 2000.

Table 1. Growth Conditions for the Deposition of Mixed-Metal Oxide Thin Films from **2** and **3**

precursor concentration (toluene)	0.2 g/25 mL
carrier gas (N_2) flow rate (cm^3/min)	25
sample injection (mL/min)	0.25
furnace temperature	300 °C for **1** and 460 °C for **2**
substrate	glass
deposition time	100 min

both cases, the anisotropic displacement parameters refine in such a way that the components of the anisotropic displacement parameters along several of the M−O and M−Cl bonds are not similar any more (i.e., the CheckCif/PLATON software, CheckCif/PLATON, operated by the International Union of Crystallography, http://journals.iucr.org/services/cif/checking/checkform.html, recognizes several level B and C "Hirschfeld test alerts").[33] No "Hirschfeld test alerts" are observed when refining an occupancy ratio as described above.

Two crystallographically independent sites with toluene solvate are found in the unit cell of **2**, one of which is located on an inversion center. The aromatic ring of the latter was restrained to resemble a regular hexagon (AFIX 66 command), the methyl C atom was restrained to have the same distance from both *o*-C atoms within a standard deviation of 0.02, and all C atoms were restrained to have the same anisotropic displacement parameter, which was restrained to be isotropic within a standard deviation of 0.1. Additional crystal data and experimental details are listed in Table 2.

Synthesis of $Ti_4(dmae)_6(\mu\text{-}OH)(\mu\text{-}O)_6Cu_6(OAc)_9\cdot H_2O\cdot 1.5(C_6H_5{-}CH_3)$ (1). A total of 1.0 g (4.60 mmol) of $Cu(OAc)_2\cdot 2H_2O$ was added to a solution of 1.33 g (3.35 mmol) of $Ti(dmae)_4$ in 15 mL of toluene at room temperature. After stirring for 2 h, the excess of $Cu(OAc)_2\cdot 2H_2O$ was eliminated by filtration through a cannula, and the reaction mixture was evaporated to dryness under reduced pressure. The solid was redissolved in 5 mL of toluene to give 95% of the crystalline product after 5 days at −10 °C. Mp: 182 °C. Anal. Calcd for $C_{52.50}H_{102}N_6O_{32}Ti_4Cu_6$: C, 33.11; H, 5.40; N, 4.41. Found: C, 33.26; H, 5.10; N, 4.33. IR: 3421br, 2886w, 1598br, 1415br, 1387br, 1335s, 1253s, 1179w, 1085s, 1018w, 951w, 895w, 785br, 669w, 612w, 371w, 319s, 284s cm^{-1}. FABMS (negative mode): *m*/*z* $[M]^-$ not found, 648 ($[Cu_3(\mu\text{-}OH)(OAc)_3(dmae)_3]^-$), 551 ($[Ti_2Cu_2(\mu\text{-}O)_4(OAc)_3(dmae)]^-$), 459 ($[Ti_2Cu_2(\mu\text{-}O)_2(OAc)_2(dmae)]^-$), 369 ($[Ti_2Cu_2(OAc)(dmae)]^-$), 274 ($[Cu_2(OAc)(dmae)]^-$), 183 ($[Ti_2(dmae)]^-$), 151 ($[Cu(dmae)]^-$). TGA: 150−300 °C single-step decomposition (residue of 39.65%).

Synthesis of $Zn_7(OAc)_{10}(\mu\text{-}OH)_6Cu_5(dmae)_4Cl_4\cdot 2(C_6H_5{-}CH_3)$ (2). A total of 2.32 g (10.63 mmol) of $Zn(OAc)_2\cdot 2H_2O$ was added to a solution of 1.0 g (5.31 mmol) of $[Cu(dmae)Cl]_4$ in 10 mL of toluene at room temperature. After stirring for 2 h, unreacted $Zn(OAc)_2\cdot 2H_2O$ was eliminated by filtration through a cannula, and the reaction mixture was evaporated to dryness under reduced pressure. The solid was redissolved in 5 mL of toluene to give 85% of the crystalline product after 3 days at −10 °C. Mp: 152 °C. Anal. Calcd for $C_{50}H_{92}N_4O_{30}Cl_4Zn_7Cu_5$: C, 27.95; H, 4.31; N, 2.60. Found: C, 27.12; H, 4.10; N, 2.60. IR: 3396br, 2965w, 2923w, 1580br, 1424br, 1342w, 1261m, 952m, 896m, 801s, 673s, 617m, 463w, 321m, 284s, 270m cm^{-1}. FABMS (positive mode): *m*/*z* $[M]^+$, not found, 864 ($[Zn_4(OAc)_5(\mu\text{-}OH)_2Cu(dmae)_2Cl_2]^+$), 555 ($[Zn_4(OAc)_5]^+$), 553 ($[Cu_4(dmae)_3Cl]^+$), 462 ($[Cu_2(dmae)_3Cl_2]^+$), 373 ($[Cu_2(dmae)_2Cl_2]^+$), 372 (369) ($[Zn_3(OAc)_3]^+$), 338 ($[Cu_2(dmae)_2Cl]^+$), 274.99 (277) ($[Cu(dmae)_2Cl]^+$), 242 (241) ($[Zn(OAc)_3]^+$), 186.99 (185) ($[Cu(dmae)Cl]^+$), 151.5 (149) ($[Cu(dmae)]^+$). TGA: 105−175 °C (12.33 wt % loss), 175−329 °C (38.92 wt % loss), 329−460 °C (residue of 43.45%).

Deposition of Thin Films. Mixed-metal oxide thin films were prepared on a glass substrate using an ultrasonic nebulizer to generate an aerosol as described elsewhere.[28] The substrate, 1.5 × 4 cm glass slide, was positioned horizontally in a glass tube in a furnace fitted with an aerosol-generating assembly. N_2 gas and sample solution flow was manually controlled. Parameters for the growth of the thin film are listed in Table 1.

Results and Discussion

A large number of homoleptic copper, zinc, and titanium alkoxides with simple aliphatic or aromatic alkoxide ligands are known.[34−36] The steric demand and coordinative flexibility of the ligand system have a great influence on the aggregation and volatility of the complexes. For example, conventional copper alkoxides usually exist as associates between two or more metal centers formed via μ-alkoxide bridges and are thus forming mostly insoluble and nonvolatile species.[37] For some homometallic alkoxides, the solubility has been improved by the use of chelating and/or sterically crowded ligands, which because of their multidentate behavior and/or steric bulk are able to reduce the association of the metal alkoxides to produce soluble derivatives.

Metal acetate and metal alkoxides/aminoalkoxides are the most used reactants for the synthesis of heterobimetallic complexes because of their bridging or bridging−chelating coordination properties. Metal alkoxides and carboxylates generally react with one another by the elimination of an ester as a volatile byproduct,[38] but in the reactions observed here, it is more likely that the oligomeric oxo and hydroxo complexes were formed through hydrolysis by water from the hydrated starting materials in combination with the loss of acetate and dmae ligands. However, such reactions can occur under very mild conditions (room temperature and nonpolar solvents), and thus the complexes can be synthesized by simple mixing of the starting materials in an appropriate solvent. The reactions between divalent metal acetates of copper and zinc with $Ti(dmae)_4$ and $[Cu(dmae)Cl]_4$ illustrate these features. These reactions proceed smoothly and quantitatively in hydrocarbon solvents over a period of 1 or 2 h with progressive dissolution of the acetate. The excess metal acetate is easily removed by filtration, and the complexes can be crystallized out almost quantitatively from the filtrate. Thus, **1** was isolated by reacting appropriate amounts of copper(II) acetate dihydrate with $Ti(dmae)_4$ in dry toluene at room temperature according to chemical equation 1. Similarly, **2** was prepared by the reaction of

(33) Hirschfeld, F. L. *Acta Crystallogr*. **1976**, *A32*, 239−244.

(34) (a) Goel, S. C.; Chiang, M. Y.; Buhro, W. E. *Inorg. Chem*. **1990**, *29*, 4646−4652. (b) Goel, S. C.; Kramer, K. S.; Chiang, M. Y.; Buhro, W. E. *Polyhedron* **1990**, *9*, 611−613.

(35) (a) Purdy, A. P.; George, C. F. *Polyhedron* **1994**, *13*, 709−712. (b) Purdy, A. P.; George, C. F.; Callahan, J. H. *Inorg. Chem.* **1991**, *30*, 2812−2819.

(36) (a) Lei, X.; Shang, M.; Fehlner, T. P. *Organometallics* **1997**, *16*, 5289−5301. (b) Lei, X.; Shang, M.; Fehlner, T. P. *Organometallics* **1996**, *15*, 3779−3781.

(37) Bradley, D. C.; Mehrotra, R. C.; Gaur, D. P. *Metal Alkoxides*; Acadenic Press: London, 1987.

(38) Boulmaaz, S.; Papiernik, R.; Hubert-Plazgraf, L. G.; Septe, B.; Vaissermann, J. *J. Mater. Chem.* **1997**, *7* (10), 2053−2061.

Table 2. Crystal Data and Structure Refinement for Compounds **1** and **2**

empirical formula	$C_{52.5}H_{102}Cu_6N_6O_{32}Ti_4$	$C_{50}H_{92}Cl_4Cu_{4.94}N_4O_{30}Zn_{7.06}$
moiety formula	$C_{42}H_{88}Cu_6N_6O_{31}Ti_4 \cdot C_7H_8 \cdot 0.5C_7H_8 \cdot H_2O$	$C_{36}H_{76}Cl_4Cu_{4.94}N_4O_{30}Zn_{7.06} \cdot 2C_7H_8$
formula weight	1902.24	2146.67
solvent	toluene	toluene
cryst habit, color	block, blue	block, blue
T (K)	90(2)	100(2)
cryst syst	triclinic	monoclinic
space group	$P\bar{1}$	$P2_1/n$
unit cell dimensions		
a (Å)	12.3480(16)	15.2973(8)
b (Å)	13.8837(18)	17.8935(9)
c (Å)	24.831(3)	15.3980(8)
α (deg)	74.618(2)	
β (deg)	84.485(2)	113.7280(10)
γ (deg)	72.854(2)	
V (Å^3)	3921.3(9)	3858.5(3)
Z	2	2
density (calcd)	1.611	1.844
abs coeff	2.058	3.732
F(000)	1954	2156
cryst size (mm^3)	0.45 × 0.40 × 0.20	0.60 × 0.50 × 0.41
θ range for data collection (deg)	1.58−26.37	1.84−28.28
index ranges	$-15 \le h \le 15$	$-20 \le h \le 20$
	$-17 \le k \le 17$	$-23 \le k \le 23$
	$-31 \le l \le 31$	$-20 \le l \le 20$
reflns collected	33 679	39 225
indep reflns	15 985	9587
abs correction	multiscan	multiscan
max and min transmission	0.663 and 0.440	0.217 and 0.129
data/restraints/param	15 985/10/921	9587/3/471
GOF on F^2	1.223	1.051
final R indices [$I > 2\sigma(I)$]	R1 = 0.0660, wR2 = 0.1564	R1 = 0.0250, wR2 = 0.0632
R indices (all data)	R1 = 0.0768, wR2 = 0.1609	R1 = 0.0277, wR2 = 0.0645
largest diff peak and hole (e Å^{-3})	+1.415 and −1.039	+0.922 and −0.442

tetrameric (*N*,*N*-dimethylamino)ethanolatocopper(II) chloride with zinc(II) acetate dihydrate in dry toluene according to chemical equation 2. Both complexes **1** and **2** were characterized by melting point, elemental analysis, FT-IR, FABMS, and single-crystal XRD. In the IR spectra, the band at 3421 cm^{-1} due to the water molecule in complex **1** is at higher frequency than the O−H absorption band of complex **2** at 3396 cm^{-1}. The difference $\Delta = \nu_{as}(CO_2) - \nu_s(CO_2)$ suggests a chelating or bridging−chelating behavior for the acetate ligands.[39] In the FABMS spectra, both complexes **1** and **2** do not show molecular ion peaks. The adamantane-like cage $Ti_4(\mu\text{-}O)_6$ of complex **1** breaks down under experimental conditions and gives multiple fragments of different *m*/*z* ratios, with the heaviest fragment observed being $[Cu_3(\mu\text{-}OH)(OAc)_3(dmae)_3]^-$, while in case of complex **2**, the largest mass fragment was $[Zn_4(OAc)_5(\mu\text{-}OH)_2Cu(dmae)_2Cl_2]^-$, thus indicating the instability of the complexes under the experimental conditions used.

$$4Ti(dmae)_4 + 6Cu(OAc)_2 \cdot 2H_2O \xrightarrow[RT]{\text{toluene}} Ti_4(dmae)_6(\mu\text{-}OH)(\mu\text{-}O)_6Cu_6(OAc)_9 \cdot H_2O \cdot 1.5(C_6H_5{-}CH_3) + 3HOAc + 4H_2O + 10(dmaeH) \quad (1)$$

$$7Zn(OAc)_2 \cdot 2H_2O + {}^5/_4[Cu(dmae)Cl]_4 \xrightarrow[RT]{\text{toluene}} Zn_7(OAc)_{10}(\mu\text{-}OH)_6Cu_5(dmae)_4Cl_4 \cdot 2(C_6H_5{-}CH_3) + 4HOAc + 8H_2O + dmaeH + HCl \quad (2)$$

Molecular Structure of 1. Complex **1** is paramagnetic and crystallizes in the triclinic space group $P\bar{1}$. Two different types of solvate toluene molecules are found in the unit cell, one of which is disordered around a center of inversion. The molecules themselves are located on general positions. Each molecule is hydrogen bonded via two water molecules to another molecule of **1** to form dimers of the type **1**···$(H{-}O{-}H)_2$···**1** arranged around the center of inversion at the origin of the unit cell. A simplified depiction of the structure of **1** is shown in Figure 1, and selected bond distances and angles are given in Tables 3 and 4. The complex is made up of six partially connected Cu units arranged around a central adamantane-like cage of $Ti_4(\mu\text{-}O)_6$. In the complex, six Cu and four Ti centers are linked together by O atoms, which are doubly/triply bridging between the metal atoms. Three of the Cu units are connected to the $Ti_4(\mu\text{-}O)_6$ unit solely via titanium atom Ti1; the other three are arranged as a rim around the $Ti_3(\mu\text{-}O)_3$ base of the adamantane cage. This effectively splits the molecule into two units only connected via one octahedral TiO_6 unit: a top unit of $Ti_1Cu_3(\mu\text{-}OH)(OAc)_3(dmae)_3 \cdot H_2O$ and a bottom unit of $Ti_4(\mu\text{-}O)_6Cu_3(OAc)_6(dmae)_3$ (see Figures 1 and 2 in the Supporting Information).

The bottom $Ti_4(\mu\text{-}O)_6Cu_3(OAc)_6(dmae)_3$ moiety of the complex is close to having noncrystallographic 3-fold symmetry with only minor deviations mainly caused by one of the solvate water molecules being hydrogen bonded to the O atom of an acetate group. The Cu−O bond of this O atom [Cu6−O17 = 2.238(4) Å] is only slightly weakened when compared to the other $Cu{-}O_{acetate}$ bonds [1.962(4) and

(39) Deacon, G. B.; Phillips, R. J. *Coord. Chem. Rev.* **1980**, *33*, 227−250.

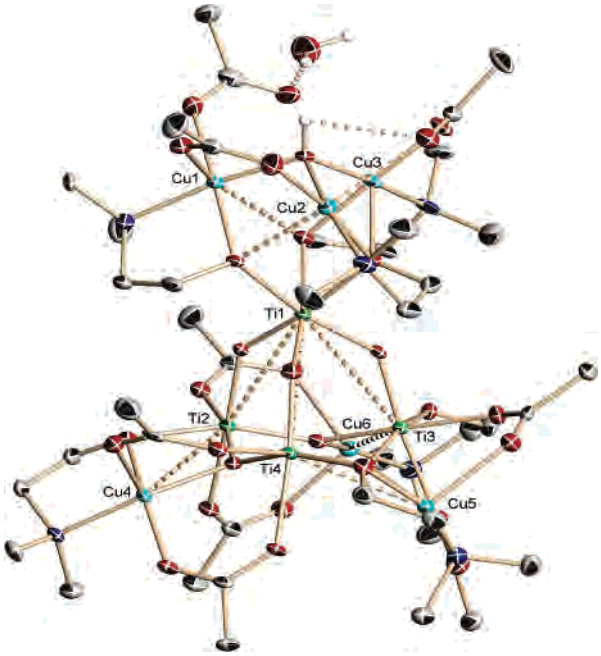

Figure 1. ORTEP drawing showing the molecular structure of **1**. Thermal ellipsoids are at the 50% probability level. Dashed lines resemble weak interactions and metal−metal interactions. Dotted lines indicate hydrogen-bonding interactions. The toluene solvate molecules as well as all but O−H hydrogen atoms are omitted for clarity.

Table 3. Selected Bond Distances (Å) for **1**

N1−Cu1	2.042(5)	O31−Cu5	1.914(4)
N2−Cu3	2.053(6)	O10−Cu3	2.370(4)
N3−Cu2	2.035(5)	O9−Cu3	1.950(4)
N4−Cu4	2.016(5)	O10−Cu2	1.950(4)
N5−Cu6	2.028(5)	O10−Cu3	2.370(4)
N6−Cu5	2.020(5)	O15−Cu4	2.203(5)
O31−Cu5	1.914(4)	O8−Ti1	2.075(4)
O8−Cu1	1.960(4)	O13−Ti1	1.862(4)
O9−Cu3	1.950(4)	O10−Ti1	2.114(4)
O10−Cu2	1.950(4)	O11−Ti1	1.871(4)
O10−Cu3	2.370(4)	O12−Ti1	1.849(4)
O15−Cu4	2.203(5)	O9−Ti1	2.069(4)
O17−Cu6	2.238(4)	O12−Ti2	1.813(4)
O19−Cu5	2.194(4)	O16−Ti2	2.048(5)
O20−Cu4	1.974(4)	O30−Ti2	1.851(4)
O21−Cu6	1.963(4)	O25−Ti2	2.137(4)
O22−Cu5	1.984(4)	O29−Ti2	1.906(4)
O24−Cu4	1.966(4)	O13−Ti3	1.793(4)
O26−Cu6	1.962(4)	O18−Ti3	2.035(4)
O28−Cu5	1.969(4)	O21−Ti3	2.028(4)
O29−Cu4	1.921(4)	O27−Ti3	2.165(4)
O30−Cu6	1.922(4)	O30−Ti3	1.919(4)
O1−Cu3	1.930(4)	O11−Ti4	1.788(4)
O3−Cu2	1.941(5)	O14−Ti4	2.044(4)
O4−Cu1	2.412(5)	O22−Ti4	2.028(4)
O5−Cu1	1.935(5)	O23−Ti4	2.163(4)
O7−Cu1	1.963(4)	O11−Ti4	1.788(4)

2.203(5) Å for Cu6−O26 and Cu4−O15, respectively], and the general 3-fold symmetry is mainly retained (see Figure 1 in the Supporting Information). The core of this subunit is built by the adamantane-like $Ti_4(\mu\text{-}O)_6$ cage, surrounded by chelating and bridging acetate and dmae ligands. The Ti−Ti distances from Ti1 to each of the other Ti atoms are significantly shorter than the Ti−Ti distances within the "cyclohexane-like" $Ti_3(\mu\text{-}O)_3$ base. The former values [3.378(15), 3.381(15), and 3.386(15) Å] are consistent with literature values for similar compounds;[40,41] the latter are all larger than 3.47 Å and above the threshold for a Ti−Ti bonding interaction.

Table 4. Selected Bond Angles (deg) for **1**

Cu1−O8−Ti1	114.2(2)	O30−Ti2−O29	92.68(18)
Cu3−O9−Ti1	108.9(2)	O13−Ti3−O31	96.30(18)
Cu2−O10−Ti1	111.91(19)	O13−Ti3−O30	93.26(18)
Ti1−O10−Cu3	93.54(16)	O31−Ti3−O30	92.14(18)
Ti4−O11−Ti1	134.8(2)	O7−Cu1−N1	172.3(2)
Ti2−O12−Ti1	134.8(2)	O3−Cu2−O7	97.12(19)
Ti3−O13−Ti1	135.7(2)	O10−Cu2−O7	85.91(18)
Cu4−O20−Ti2	94.71(17)	O3−Cu2−N3	92.4(2)
Cu6−O21−Ti3	95.68(17)	O10−Cu2−N3	85.2(2)
Ti4−O29−Ti2	134.4(2)	O7−Cu2−N3	170.0(2)
Ti4−O29−Cu4	120.9(2)	O1−Cu3−O7	95.36(18)
Ti2−O29−Cu4	101.30(19)	O9−Cu3−O7	86.76(17)
Ti2−O30−Ti3	134.3(2)	O1−Cu3−N2	92.1(2)
Ti2−O30−Cu6	122.0(2)	O7−Cu3−N2	169.6(2)
Ti3−O30−Cu6	100.75(18)	O29−Cu4−O20	80.59(17)
Ti3−O31−Cu5	121.9(2)	O24−Cu4−O20	165.30(18)
Ti3−O31−Ti4	134.3(2)	O29−Cu4−N4	158.5(2)
Cu5−O31−Ti4	100.50(19)	O31−Cu5−O28	95.47(18)
O12−Ti1−O13	95.64(18)	O31−Cu5−O22	79.48(17)
O12−Ti1−O11	94.95(18)	O31−Cu5−N6	160.49(19)
O13−Ti1−O11	94.60(18)	O30−Cu6−O26	96.79(18)
O12−Ti2−O30	95.75(18)	O30−Cu6−O21	80.38(17)
O12−Ti2−O29	94.05(18)	O30−Cu6−N5	159.8(2)

The top $Ti_1Cu_3(\mu\text{-}OH)(OAc)_3(dmae)_3\cdot H_2O$ moiety has no noncrystallographic symmetry. The unit can be seen as a $TiCu_3O_4$ cube, with three Cu−O bonds being significantly elongated or broken [Cu1−O9 = 2.560 Å, Cu2−O8 = 2.535 Å, and Cu3−O10 = 2.370 Å]. This results in all three Cu atoms having a square-planar coordination environment with four tightly bonded ligands (each with three O donors and one N donor), augmented by two additional weakly or nonbonded axial O ligands. All Cu atoms are tightly bonded to the μ-hydroxyl anion at the very top of the molecule, to one acetate ligand each, one dmae O atom, and one dmae N atom, but the number of Cu atoms connected to specific dmae and acetate O atoms varies. One dmae O atom bridges the Ti atom to two Cu atoms; the other two are bridging Ti1 to only one Cu atom each. One of the acetate moieties is a chelating ligand bridging Cu1 and Cu2; the other two acetate groups are bonded only to one Cu atom, a coordination mode not observed very often but previously described for other mixed-metal complexes with aminoalcohol and acetate ligands if the uncoordinated acetate O atom is stabilized by hydrogen bonding.[42] In compound **1**, one of the uncoordinated acetate O atoms is hydrogen-bonded to the water molecule; the other is weakly hydrogen-bonded to the μ-hydroxyl anion at the very top of the complex.

Molecular Structure of 2. The structure of **2** is shown in Figure 2, and selected bond distances and angles are given in Table 5. The complex is paramagnetic and crystallizes in the monoclinic space group $P2_1/n$ with two molecules of the complex as well as four solvate toluene molecules per unit cell. Each of the complex molecules is located on a

(40) Babcock, L. M.; Day, V. W.; Klemperee, W. G. *J. Chem. Soc., Chem. Commun.* **1987**, 858−859.
(41) BjiSrgvinsson, M.; Halldorsson, S.; Arnason, I. R.; Magull, J.; Fenske, D. *J. Organomet. Chem*. **1997**, *544*, 207−215.
(42) Werndrup, P.; Gohil, S.; Kessler, V. G.; Kritikos, M.; Hubert-Pfaltzgraf, L. G. *Polyhedron* **2001**, *20*, 2163−2169.

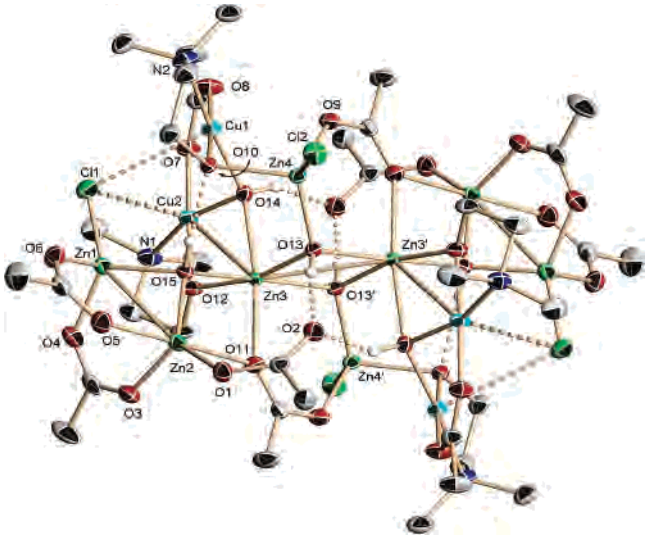

Figure 2. ORTEP drawing showing the molecular structure of **2**. Thermal ellipsoids are at the 30% level. Atoms labeled as Zn3 and Zn3′ are occupied either by Zn or by Cu with a refined ratio of 0.47(4):0.53(4). Symmetry operation: #1, $-x, -y, -z + 1$. The toluene solvent molecules as well as all but the hydroxyl H atoms are omitted for clarity. Dotted lines indicate hydrogen bonds. Dashed lines indicate close Cu···Cl contacts.

crystallographic inversion center; the toluene molecules are located in general positions. The structure can be described as being made up of two asymmetric units related by a crystallographic inversion center located in the middle of the molecule. The two asymmetric units are covalently connected via each two doubly bridging μ-hydroxyl groups and two chelating−bridging acetate ligands. In the asymmetric part of the molecule, three Zn atoms, two Cu atoms, and one disordered metal site with mixed Zn and Cu occupation are linked by bridging O dmae groups, chelating−bridging O atoms of acetate ligands, and doubly bridging μ-hydroxyl anions. All of the three types of ligands span a range of different coordination modes. The acetate ligands either are chelating two metals, are chelating−bridging three metal atoms, or are covalently bonded to a Zn atom and hydrogen-bonded to two μ-hydroxyl groups, an unusual but not unheard of coordination mode for acetate ligands, as was already discussed for compound **1**. The dmae groups are chelating−bridging two metals, and one O atom is further hydrogen-bonded to one of the μ-hydroxyl anions.

Both of the Cu atoms have a distorted square-pyramidal geometry with a O_3N donor set, and the environments of two of the three Zn atoms can be best described as a distorted tetrahedron with a ZnO_3Cl core, while the third Zn atom has distorted trigonal-bipyramidal ZnO_5 geometry.

The last site occupied by metal atoms in **2** is partially occupied by Zn and partially by Cu, with an approximate occupancy ratio of 1:1 (Zn3/Cu3). The overall geometry around Zn3/Cu3 is a distorted octahedron of six O atoms. The Zn3/Cu3−O bond distances are larger than those for the tetrahedral Zn1 and Zn2 centers but are in good agreement with those observed for octahedral $[Zn(acac)_2(dmaeH)]$.[43]

(43) Mazhar, H.; Zeller, M.; Mazhar, M.; Hunter, A. D.; Asif, A. *Acta Crystallogr*. **2005**, *E61*, m1539−m1541.

Table 5. Selected Bond Distances (Å) and Angles (deg) for **2**

bond distance (Å)		bond angles (deg)	
Cl1−Zn1	2.2418(5)	O14−Cu1−O8	93.37(6)
Cl2−Zn4	2.1962(5)	O14−Cu1−O10	92.29(5)
Cu1−O14	1.9260(13)	O14−Cu1−N2	174.55(7)
Cu1−O10	1.9609(13)	O10−Cu1−N2	86.17(6)
Cu1−N2	2.0148(17)	O12−Cu2−O14	85.04(6)
Cu2−O12	1.9110(14)	O12−Cu2−N1	86.25(6)
Cu2−O14	1.9725(13)	O14−Cu2−N1	164.66(7)
Cu2−N1	2.0156(17)	O12−Cu3−O15	86.68(6)
Cu3−O12	1.9984(14)	O12−Cu3−O13	166.28(5)
Cu3−O15	2.0237(13)	O15−Cu3−O13	87.07(5)
Cu3−O13	2.1154(13)	O12−Cu3−O11	96.96(5)
Cu3−O11	2.2161(14)	O15−Cu3−O11	81.13(5)
Cu3−O14	2.2324(13)	O13−Cu3−O11	94.12(5)
Zn1−O15	1.9737(13)	O12−Cu3−O14	76.47(5)
Zn2−O15	1.9689(13)	O15−Cu3−O14	94.53(5)
Zn2−O11	2.3216(14)	O13−Cu3−O14	91.88(5)
Zn4−O13	1.9518(13)	O11−Cu3−O14	172.40(5)
Zn4−O10	2.0077(13)	O15−Zn2−O11	79.65(5)
Cu3−Zn3#1	3.0654(4)	O15−Zn2−O11	79.65(5)
Zn1−Zn2	3.0421(4)	O13−Zn4−O10	101.79(5)
		O9−Zn4−O10	95.93(6)
		O10−Zn4−Cl2	110.83(4)
		O15−Zn2−O11	79.65(5)
		O9−Zn4−Cl2	112.88(4)
		O10−Zn4−Cl2	110.83(4)
		O4−Zn1−Cl1	120.45(5)
		O15−Zn1−Cl1	114.91(4)
		O6−Zn1−Cl1	106.12(5)
		O13−Zn4−Cl2	122.41(4)

Singly based on the diffraction data, it is not possible to decide if the distribution of Zn and Cu of this site is random, i.e., some of the molecules would have two each of Cu or Zn atoms, or if it is systematic, i.e., every molecule has exactly one Cu and one Zn atom at each of the two positions. Also ionic radii for Cu^{II} (0.88) and Zn^{II} (0.87) in an octahedral environment are very similar.[44] In favor of an ordered 1:1 ratio for each molecule is the close proximity of the two crystallographically dependent sites of Zn3/Cu3. They are located close to the center of inversion, and the two metal atoms are connected both via two bridging hydroxyl groups (O13 and O13′) and via a direct metal−metal contact of 3.0654(4) Å. Thus, a direct communication between the two sites can be assumed, which might lead to an ordered 1:1 ratio for each single molecule. A similar disorder of a metal site was previously reported by Hubert-Pfaltzgraf and co-workers for the compound $[Ni(Ni_{0.25}Cu_{0.75})_2(\mu_3\text{-OH})(\mu\text{-OAc})(\eta^1\text{-OAc})_2(\mu,\eta^2\text{-ORN})_2(\eta^2\text{-R}^N\text{OH})]$ [R^N-OH = $(CH_3)_2N(CH_2)(CHOH)(CH_3)$].[42] In this complex, which can be seen as a simpler but related mixed-metal analogue of **2**, two metal sites were each occupied by 75% Cu and 25% Ni, which was justified by the coexistence of two molecules with different compositions with a metal ratio of $CuNi_2$ and Cu_2Ni, respectively, similar to the one found for complex **2**. For complex **2**, the single-crystal XRD results were further supported by the atomic absorption spectroscopic analysis, giving a Zn/Cu metal ratio of 1.4:1, which is in good agreement with the refined value found by single-crystal XRD.

Thermal Decomposition Studies and Characterization of Thin Films. The thermal behavior (Figure 3) of complexes

(44) Shannon, R. D. *Acta Crystallogr*. **1976**, *A32*, 751.

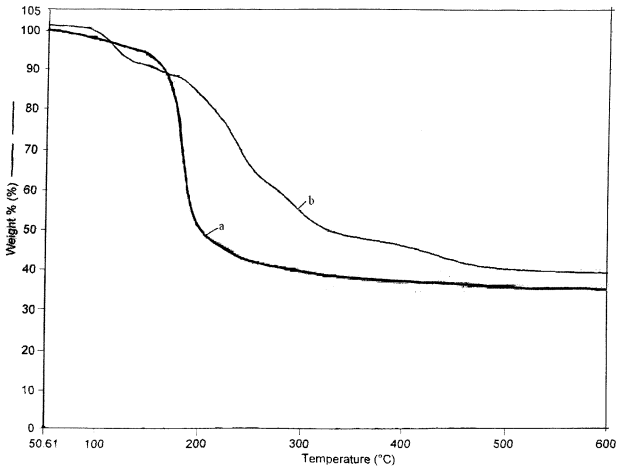

Figure 3. TGA plot showing loss in weight with an increase in the temperature (a) for complex **1** and (b) for complex **2**.

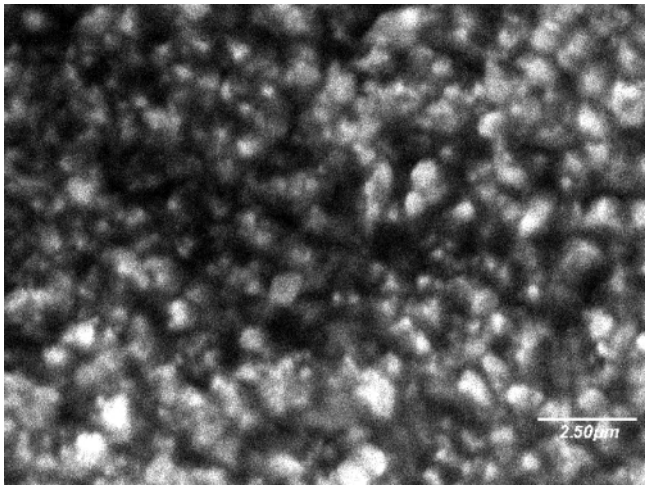

Figure 4. SEM micrograph of an oxide film deposited from complex **1** at 300 °C.

1 and **2** has been examined by TGA, performed under an inert atmosphere of flowing N_2 gas (25 mL/min) and a heating rate of 10 °C/min. The TGA pattern of compound **1** shows a single weight loss step starting at about 150 °C, with a maximum weight loss at 180 °C. The decomposition ends at about 300 °C, leaving a residue of 39.65% of the initial mass, slightly less than 40.12% calculated for complete conversion to a $Cu_6Ti_4O_{12}$ composite. The TGA curve of complex **2** shows three stages of weight loss. The first step begins at 105 °C and is completed at 175 °C. The second one starts at 175 °C and is completed at 329 °C, which is directly followed by the last stage ranging from 329 °C to about 460 °C, resulting in a residue amounting to 43.45% of the initial weight. The residual weight (43.45%) is less than but close to the expected composition for $Cu_5Zn_7O_{12}$ (45.0%), the presence of which was further supported by the XRD analysis of the residue (see below).

The films exhibit a good adhesion to the substrate, as verified by the scotch tape test, and are stable toward air and moisture. They reflect light in multishaded colors depending upon the particle size and thickness of the deposited film. The SEM image (Figure 4) of an oxide thin film deposited from complex **1** shows film morphology with small crystallites evenly distributed with no preferred orientation and grains having a variable shape without well-defined boundaries. The SEM image (Figure 5) of an oxide thin film deposited from complex **2** shows compact and smooth film morphology with homogenously dispersed particles and grains that are well-defined with clear boundaries.

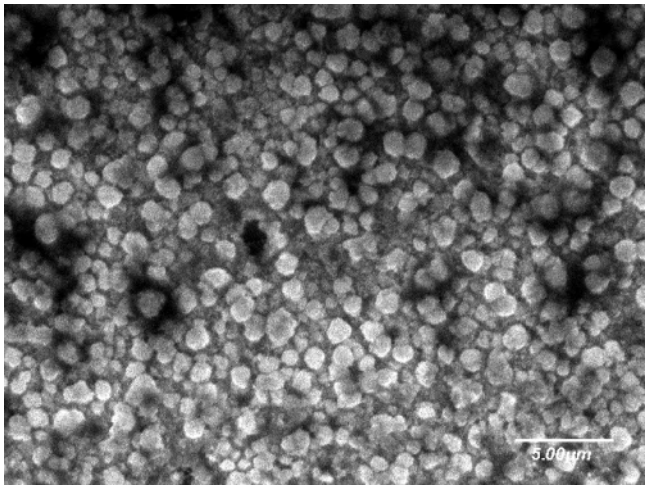

Figure 5. SEM micrograph of an oxide film deposited from complex **2** at 460 °C.

The energy-dispersive X-ray (EDX) analysis indicates that the metallic ratio of Cu/Ti in complex **1** is close to 1.5:1 while that of Cu/Zn in complex **2** is found to be 1:1.4. The EDX analyses also prove the clean decomposition of the complexes without incorporation of impurities from either the organic part of the complexes or the carrier gas and the formation of a pure ceramic oxide.

The X-ray diffractograms of the films obtained from complexes **1** and **2** (see Figures 3 and 4 in the Supporting Information) indicate the formation of distinct oxide mixtures according to eqs 3 and 4.

$$Ti_4(dmae)_6(\mu\text{-}OH)(\mu\text{-}O)_6Cu_6(OAc)_9\cdot H_2O\cdot (C_6H_8)_2 \xrightarrow{300\ °C} 2Cu_3TiO_4 + 2TiO_2 \quad (3)$$

$$Zn_7(OAc)_{10}(\mu\text{-}OH)_6Cu_5(dmae)_4Cl_4 \xrightarrow{460\ °C} 7ZnO + 5CuO \quad (4)$$

In the case of complex **1**, the XRD peak pattern indicates the presence of Cu_3TiO_4[45]and TiO_2[46] in a ratio of 0.77:0.23. Copper titanium oxide (Cu_3TiO_4) and anatase have the hexagonal and tetragonal space groups $P63/mmc$ and $I4_1/amd$, respectively. It has been reported that dielectric properties[47] and the quality factor[48] of titanium(IV) oxide based ceramics deteriorate because of the reduction of Ti^{4+} to Ti^{3+} during solid-state synthesis. Hence, complex **1**, which

(45) (a) ICDD powder diffraction database file card number 01-071-1995. (b) Hayashi, K.; Mizutani, N.; Kato, M. *J. Chem. Soc. Jpn.* **1974**, *1*, 6.
(46) ICDD powder diffraction database file card number 01-071-1167.
(47) Nomura, S.; Toyama, K.; Kaneta, K. *Jpn. J. Appl. Phys.* **1983**, *22*, 1125−1128.
(48) Popov, S. G.; Levitskii, V. A. *J. Solid State Chem.* **1981**, *38*, 1−9.

decomposes at a temperature as low as 300 °C, may prove to offer a facile synthetic route to copper titanium oxides with Ti in oxidation state IV.

In the case of complex **2**, the oxide phases detected are ZnO[49] and CuO.[50] The major crystalline oxide phase is hexagonal ZnO in the space group *P*63*mc*, and CuO is found in the form of *syn*-tenorite in the monoclinic space group *C*2/*c*.

Conclusion

The present investigations are focused on the easy preparation of single-source heterobimetallic complexes having a high solubility and stability and that can be easily decomposed to a homogeneous mixed-metal oxide composite in a single step. The heterobimetallic complexes **1** and **2** are synthesized by simple and routine chemical reactions of Ti(dmae)$_4$ with Cu(OAc)$_2$·2H$_2$O for **1** and [Cu(dmae)Cl]$_4$ with Zn(OAc)$_2$·2H$_2$O for **2**, both under very mild conditions in toluene as the solvent. Structural and spectroscopic studies confirmed the identity of the compounds, which are highly soluble in organic solvents, are stable under standard conditions, and are reasonably volatile. The thermal decomposition studies of **1** showed that the general idea of combining a Cu precursor moiety with Ti moieties in a single molecule results in a copper titanium oxide in a single step at 300 °C. Similarly, complex **2** decomposes to give a Cu/Zn mixed-metal oxide material in single-step decomposition at 460 °C. Further studies of this and related systems can now open new approaches to the synthesis of nanoparticles with controlled geometries, which, in turn, might find use in advanced technological and industrial applications.

Acknowledgment. M.H., A.A.T., and M.M. acknowledge the "Higher Education Commission and Pakistan Science Foundation Islamabad, Pakistan" for financial support through the "Merit Scholarship Scheme for PhD Studies in Science & Technology (200 Scholarships)" and Project No. PSF/R&D/C-QU/CHEM.(218). The Smart Apex diffractometer was funded by NSF Grant 0087210, by Ohio Board of Regents Grant CAP-491, and by Youngstown State University.

Supporting Information Available: X-ray crystallographic files in CIF format, ORTEP drawings of **1**, and X-ray diffractograms of **1** and **2**. This material is available free of charge via the Internet at http://pubs.acs.org.

IC0624470

(49) (a) ICDD powder diffraction database file card number 01-076-0704. (b) Schulz, H.; Thiemann, K. H. *Solid State Commun.* **1979**, *32*, 783−785.

(50) (a) ICDD powder diffraction database file card number 00-005-0661. (b) Hanawalt, J. D.; Rinn, H. W.; Frevel, L. K. *Ind. Eng. Chem., Anal. Ed.* **1938**, *10*, 457−512.